# Effect of Exchange–correlation Functionals on Ground State Geometries, Optoelectronic and Charge Transfer of Triphenylamine-based Dyes

Malak Lazrak [a], Hamid Toufik* [a], Sliman Ennehary [a], Si Mohamed Bouzzine [a,b] and Fatima Lamchouri [a]

The importance of the Density Functional Theory (DFT) calculation approach lies in their ability to provide a highly accurate prediction of structural and optoelectronic properties. However, the traditional methods of DFT failed to predict optoelectronic properties satisfactorily. Therefore, it will be necessary to examine methods containing different percentages of Hartree-Fock exchange and correlation in order to find the most suitable functionals. DFT and Time-Dependent-DFT (TD-DFT) calculations was carried out using four different functionals approximations incorporating a different amount of Hartree Fock exchange (B3LYP, BHandHLYP, CAM-B3LYP and LCωPBE), in order to evaluate their accuracies to predict the geometrical, optoelectronic and charge transfer properties of four triphenylamine-based dyes for Dye-Sensitized Solar Cells (DSSCs) applications. The functional hybrid B3LYP was the best among adopted functional that reproduced the geometrical, optoelectronic and charge transfer properties. On the other hand, it has been shown that the Hartree-Fock exchange percentage for BHandHLYP, significantly improved TD-DFT results in the case of organic dyes. Moreover, the corrected long-range functionals (CAM-B3LYP and LC-wPBE) present valuable tools for giving results of comparable precision with experimental optical data. In terms of the choice of the most appropriate functional for computational calculation, the obtained results can be useful for future DSSC applications.

Graphical abstract
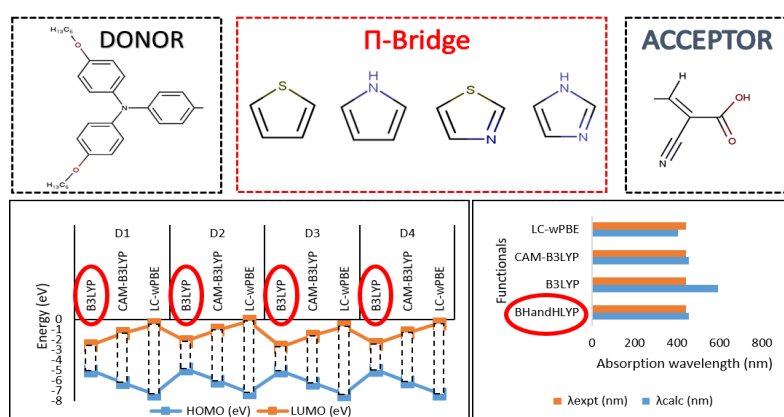
1. Introduction

Computational modeling of organic molecules has been   widely used for the design of materials such as organic

ᵃ Laboratory of Natural Substances, Pharmacology, Environment, Modeling, Health and Quality of Life (SNAMOPEQ), Polydisciplinary Faculty of Taza, Sidi Mohamed Ben Abdellah University, B.P. 1223, Taza Gare, Taza, Morocco. ᵇ Regional Center for Training and Professional Education, BP 8, Errachidia, Morocco. Corresponding author. E-mail: **hamid.toufik@usmba.ac.ma**

photovoltaics (OPVs) [1, 2], organic light emitting diodes (OLEDs) [3−6] and organic dyes for dye-sensitized solar cells (DSSCs) [7−11]. In this context, the Density Functional Theory (DFT) is today one of the most widely used methods in quantum calculations of the electronic structures for its reliable accuracy, low computational cost and its compatibility with experimental results [12]. The DFT finds its origins in the model developed by Lewellyn Thomas and Enrico Fermi at the end of the 1920s [13]. However, it was in the mid-1960s that Pierre Hohenberg, Walter Kohn and Lu Sham established the theoretical formalism on which the current method is based [14]. The idea behind Kohn and Sham was to separate the kinetic energy into two parts, one of which can be calculated exactly, T_S, and the other appears to be a small correction to bring to the energy. In this second term, appears then the electronic correlation. The total energy DFT is written as:

$$E_{DFT}(\rho) = T_s(\rho) + E_{Ne}(\rho) + J(\rho) + E_{XC}(\rho)$$

With $T_s(\rho)$ representing kinetic energy, $E_{Ne}(\rho)$ representing the energy of electrostatic interactions between cores and electrons and $J(\rho)$ representing Coulomb energy.

The DFT energy (E_{DFT}) will reach the exact energy if and only if the exchange-correlation energy (E_{XC}) is calculated exactly. The goal of recent developments within the framework of Density Functional Theory methods is therefore to calculate this exchange-correlation part as well as possible.

Several approximations of the XC functional have been developed and tested in recent decades. The local density approximation or LDA is the first approximation that has been considered [15], it consists in considering the exchange-correlation potential of the solid by that of a homogeneous gas of free electrons. Admittedly, this approach may seem justified for a metal but in the case of semiconductors, the exchange-correlation potential presents a discontinuity when adding or removing an electron to the system, which will systematically lead to erroneous gaps.

To improve the accuracy of DFT calculations, some authors have had the idea of defining a density functional that they associated with its own derivatives in order to take into account the system's non-uniformity [16−18]. In general, the approximation of the generalized gradient or GGA improves a certain number of properties like total energy or cohesion energy, but does not lead to a precise description of all the properties of a semiconductor material [19]. The most popular GGA functionals include the B88 exchange functional of Becke [17] and the "non-empirical" exchange−correlation functionals PW919 and PBE proposed by Perdew and co-workers [20].

Since the 1990s, a new approach has appeared that of hybrid functionals, it approximates to the exchange-correlation functional, used within the density functional theory (DFT). The characteristic of these functionals is to have an exchange part based on the Hartree-Fock (HF) method dependent on orbitals. Moreover, the hybrid functionals aim to correct the self-interaction error of the classical approximations of the DFT (LDA and GGA) and other various DFT problems, such as problems of van der Waals bonding and Rydberg excitation energies and oscillator strengths in TDDFT calculations [21]. This approach is based on the introduction of an HF exchange, which can a priori be done by substituting the exchange part of the functional. This is accomplished using a modified two-electron HF exchange Coulomb potential $O^{HF}(r_{12})$, it's defined through the decomposition of the Coulomb potential, $1/r_{12}$, of the exchange energy as [21]:

$$\frac{1}{r_{12}} = O^{HF}(r_{12}) + \left[\frac{1}{r_{12}} - O^{HF}(r_{12})\right]_{DFT}$$

$$O^{HF}(r_{12}) = \frac{erf(\mu r_{12})}{r_{12}}$$

where $r_{12} = |r_1 − r_2|$ is the distance between electrons r_1 and r_2 and μ is a parameter that defines the proportion between HF and DFT.

Therefore, this work aims to establish a reasonable computational approach for four choosing triphenylamine-based dyes with D-π-A (electron donor - π spacer - electron acceptor) molecular structure. The π-bridge consists of four heterocycle rings, which are thiophene, pyrrole, thiazole and imidazole. On the acceptor side of this dye, the acceptor moiety is employed which contains the cyanoacrylic acid group as an electron withdrawing group and anchoring unit to attach the dye onto the TiO_2 semiconductor (Fig. 1). In this study, to explore the effect of functionals on geometries and optoelectronic properties, as well as evaluation of their accuracy on the charge transfer properties, different XC functionals was used to theoretically simulate and calculate the properties of sensitized dyes, and the calculation results were used as a guide to compare the experimental results. The usual hybrid functionals occupy a privileged position in the molecular applications of DFT. They are currently the only ones able to provide results closest to experimental data [22]. Their construction, justified by arguments relating to the adiabatic connection, includes a fixed percentage, between 20% and 25% depending on the case, of HF exchange added to a counterpart using a usual exchange function. The success of hybrid functionals (mainly B3LYP) is often associated with a partial reduction of the self-interaction error (SIE), without destroying the balance between the exchange part and the correlation part.
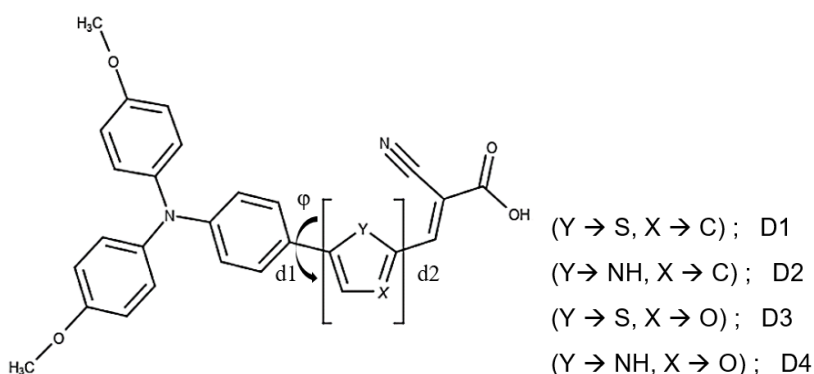

(Y → S, X → C) ; D1

(Y → NH, X → C) ; D2

(Y → S, X → O) ; D3

(Y → NH, X → O) ; D4

Fig. 1. Molecules structures and abbreviated notations of D1, D2, D3 and D4 investigated dyes.

According to previous works, BHandHLYP and CAM-B3LYP functionals showed good performance for calculating optical properties [23, 24]. Hence the choice of these two functional, in order to improve the previous results and to choose the model which can reliably describe the maximum absorption [25]. In addition, the corrected long-range LC-ωPBE was selected for the reason that it reproduces intriguing results in many cases. We note that in the case of the functionals CAM-B3LYP and LCωPBE, by using the generalized parametrization of the coulomb interaction operator, we find that both the HF exchange and the DFT counterpart are incorporated over the entire range [24].

2. Computational Methods

All calculations were performed with the Gaussian 09 program [26]. The geometrical, electronic and charge transfer properties of triphenylamine-based dyes is carried out using different functional approximations, such as the hybrid GGAs B3LYP functional, which contain 20% of HF exchange amount [27] and the long-range-corrected version CAM-B3LYP [28], where the amount of exact exchange grows with increasing interelectronic distance (From 20 to 65%). The long range corrected LC-ωPBE have, also, been tested [29, 30] (the fraction of exact exchange vary with the inter-electronic distance from 0 to 100%). The 6-31G(d,p) basis set was used for optimizing structural and electronic properties. For the optical parameters, we used the functionals mentioned above, and the BHandHLYP functional, which include 50% fraction of HF exchange and 50% of Becke88 exchange [24]. The effect of these four different functionals on optical properties were discussed using 6-31G+(d) basis sets. According to the available experimental results, the UV–Vis absorption spectra were simulated in tetrahydrofuran (THF) solvent via the conductor polarizable continuum model (CPCM).

3. Results and Discussion

3.1 Optimized geometric structures

To study the effect of different XC-functional on the linking conjugation character and planarity order between the various parts of the studied dyes. Fig. 2 displays the selected Carbon-Carbon (C-C) bond lengths between the donor and the π-bridge (d1), and between the π-bridge and the acceptor (d2) in studied dyes. Also, the dihedral angles (φ), between the donor and the π-bridge in studied compounds are illustrated in Fig. 3.

The optimized values of the selected geometrical parameters have been obtained by B3LYP, CAM-B3LYP and LC-ωPBE functionals using 6-31G(d, p) basis set.

As shown in Fig. 2, the value given by the bond lengths d2 connecting the pyrrole and imidazole π-bridges to the acceptor cyanoacrylic acid group is low compared to the bond lengths d2 connecting the acceptor cyanoacrylic acid group with the thiophene and thiazole π-bridges. This is due to the strong conjugation between the nitrogen-based π-bridges and the acceptor cyanoacrylic acid moiety when compared with the sulfur-based π-bridges [24]. We note that the diminution of the percentage of HF exchange amount contribution in the functional, according to XC, from 100% (LC-ωPBE) to 65% (CAM-B3LYP) to 20% (B3LYP), is linked to a shortening of bond length values d1 and d2.

Fig. 3 presents the values of the dihedral angles between the phenyl ring of the TPA donor and the π-bridges rings,

optimized by different selected functionals. As shown in the case of bond lengths, the decrease of the percentage of HF exchange amount contribution in the functional, according to XC, from 100% (LC-ωPBE) to 65% (CAM-B3LYP) to 20% (B3LYP), is linked to a decrease in the dihedral angles values. This implies that the small percentage of HF exchange amount contribution in the functional is manifested by a more planar structure between the phenyl ring of TPA donor and the π-bridge rings.
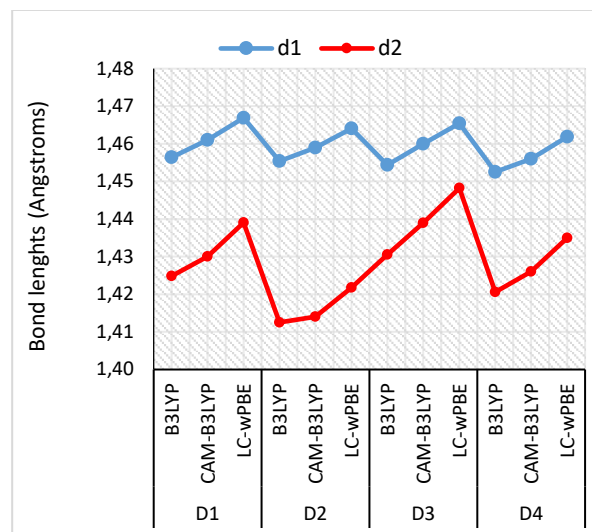

Fig. 2. Bond length d1 and d2 values for D1, D2, D3 and D4 studied dyes, calculated using B3LYP, CAM-B3LYP and LC-wPBE functionals with 6-31G(d, p) basis set.
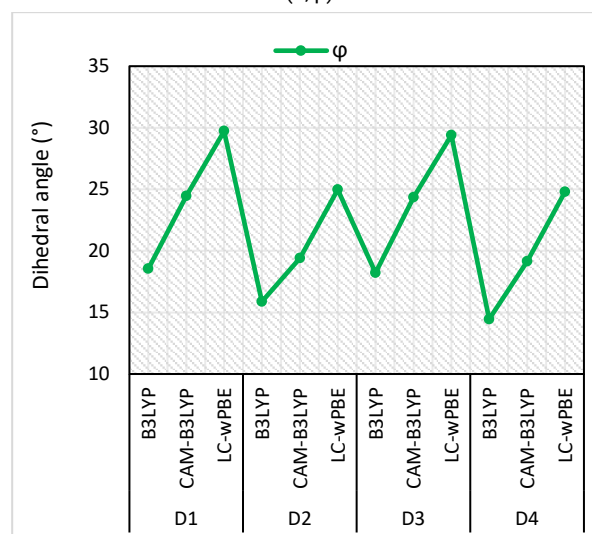

Fig. 3. Dihedral angle φ values for D1, D2, D3 and D4 studied dyes, calculated using B3LYP, CAM-B3LYP and LC-wPBE functionals with 6-31G(d, p) basis set.

It is clearly seen from these results that B3LYP hybrid functional is found to be most stable in performing structural properties [31], compared to Long-range corrected functionals (LC-wPBE and CAM-B3LYP), which account the non-Coulomb part of exchange functionals .

The B3LYP hybrid functional (Becke 3-parameter Lee-Yang-Parr) is a three-parameter functional combining the local exchange, Becke exchange and HF exchange (exact) functionals, with local correlation functionals and corrected for the Lee, Yang and Parr gradient [32]. The introduction of exact exchange then improves the results calculations, which

explains the extensive use of this functional in computational chemistry and its reliability for ground state geometry optimizations.

3.2 Electronic properties

The experimental energy values for the gap energy of the dye D1 are estimated at 2.38 eV. In the present study, several functionals are employed to calculate the frontier molecular orbital energies of studied dyes. The obtained results are given in Table 1. Energy gap value obtained from B3LYP functional for D1 dye is 2.46 eV. This calculated value is in excellent agreement with the experiment one, by less than 0.08 eV deviation from the experimental value.

Fig. 4 compares the calculated frontier molecular orbital energy levels of the triphenylamine-based dyes employing different functional. We note that the HOMO-LUMO gap of the dyes increases from 2.46 eV in D1 for B3LYP to 4.80 eV CAM-B3LYP and 6.82 eV for LC-wPBE. This significative difference is due to the fact that the DFT functionals have different amounts (α) of HF exchange in the exchange-correlation functional, that is, B3LYP (20%), CAM-B3LYP (20-65%), and LC-wPBE (0-100%). With the increasing component of HF exchange in the functional, the band gap increases, so LC-wPBE gives the longest band gap and B3LYP gives the shortest band gap.

Table 1. Energy levels of HOMO, LUMO and E_{gap} (all in eV) of studied dyes, calculated using B3LYP, CAM-B3LYP and LC-wPBE functionals with 6-31G(d, p) basis set.

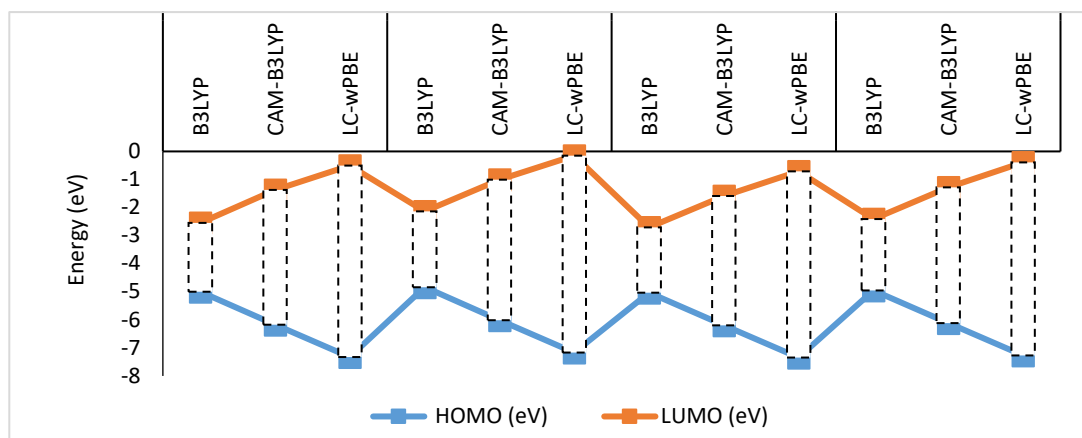| Dyes	Functionals	HOMO	LUMO	E_{gap}
D1	B3LYP	-5.00	-2.55	2.46
	CAM-B3LYP	-6.18	-1.37	4.80
	LC-wPBE	-7.33	-0.51	6.82
	Expt.	-	-	**2.38**
D2	B3LYP	-4.83	-2.13	2.70
	CAM-B3LYP	-6.01	-1.01	5.00
	LC-wPBE	-7.17	-0.15	7.02
D3	B3LYP	-5.04	-2.71	2.33
	CAM-B3LYP	-6.20	-1.59	4.61
	LC-wPBE	-7.34	-0.70	6.64
D4	B3LYP	-4.95	-2.41	2.54
	CAM-B3LYP	-6.12	-1.28	4.84
	LC-wPBE	-7.27	-0.39	6.88

Fig. 4. Gap energy, HOMO and LUMO energies levels for studied compounds, calculated using B3LYP, CAM-B3LYP and LC-ωPBE functionals with 6-31G(d, p) basis set.

3.3 Charge transfer

In order to study the effect of the functionals on the charge transfer properties of the studied dyes, Table 2 presents the adiabatic and vertical values of IP and EA, calculated using B3LYP, CAM-B3LYP and LC-ωPBE functionals.

The results show that the calculated IPa and IPv decreases, as HOMO energy, in the same following order D3 > D1 > D4 > D2. This indicates that the -NH and -CH groups in the π-bridge of D2, favor the generation of free electrons, compared to the C=S and C=O groups, in D3 compound. We also noted that the calculated EAa and EAv increases in the same trend as LUMO energy: D2 < D4 < D1 < D3,

suggesting that the C=S and C=O electron-withdrawing bridged groups in D3, favor the generation of free holes more than the -NH and -CH electron bridged groups in D2.

Other charge transfer parameters are studied, which are electron, hole and total reorganization energies. They can be determined by the equations follows [33]:

$$\lambda^+ = [E(M^-) - E^-(M^-)] - [E(M) - E^-(M)]$$
$$\lambda^- = [E^+(M) - E(M)] - [E^+(M^+) - E(M^+)]$$
$$\lambda = \lambda^+ + \lambda^-$$

The reorganization energies (λ^+ and λ^-) of triphenylamine-based dyes are calculated and are given in Table 2. It is well-known that a lower reorganization energy means a higher

charge transfer rate. The calculated electron reorganization energies (λ^+) of studied dyes with B3LYP functional are 0.233, 0.226, 0.260 and 0.246 eV for D1, D2, D3 and D4, respectively. The λ^+ of D2 and D4 are smaller than that of D1 and D3, respectively, which means that the −NH substituent decreases reorganization energies of D2 and D4. On the other hand, the λ^+ of D1 and D2 are smaller than that of D3 and D4, respectively, which means that the substitution of the carbon atom by the oxygen atom in the π-bridge increases reorganization energies. The hole electron energies (λ^-) of the studied dyes are in the same trend as electron reorganization energies.

As illustrated in Fig. 5, the charge transfer calculations show that the long-range corrected density functionals (CAM-B3LYP and LC-wPBE), overestimate the reorganization energies unlike the B3LYP hybrid functional, which has been used successfully to calculate the charge transfer parameters as for the structural and electronic properties of the studied molecules. This functional is obtained using short-range HF and long-range DFT, and such hybrid functionals are known to improve ground state properties such as geometries, band gaps and charge transfer properties in DFT calculations.

Table 2. Calculated reorganization energies, adiabatic/vertical ionization potentials and electron affinities (all in eV) of studied dyes, calculated using B3LYP, CAM-B3LYP and LC-wPBE functionals with 6-31G(d, p) basis set.

Functionals	IPa	IPv	EAa	EAv	λ^+	λ^-	λ
D1							
B3LYP	5.992	6.116	1.4	1.138	0.233	0.519	0.752
CAM-B3LYP	6.203	6.371	1.362	1.035	0.317	0.655	0.972
LC-wPBE	6.462	6.649	1.5	1.128	0.365	0.760	1.125
D2							
B3LYP	5.852	5.969	1.001	0.752	0.226	0.495	0.721
CAM-B3LYP	6.075	6.234	0.958	0.654	0.302	0.604	0.906
LC-wPBE	6.346	6.531	1.107	0.765	0.354	0.684	1.038
D3							
B3LYP	6.041	6.176	1.577	1.313	0.260	0.530	0.790
CAM-B3LYP	6.221	6.401	1.549	1.209	0.344	0.685	1.029
LC-wPBE	6.473	6.669	1.672	1.285	0.385	0.785	1.170
D4							
B3LYP	5.97	6.098	1.234	0.979	0.246	0.512	0.758
CAM-B3LYP	6.167	6.340	1.209	0.890	0.327	0.635	0.963
LC-wPBE	6.425	6.620	1.353	0.991	0.376	0.723	1.098
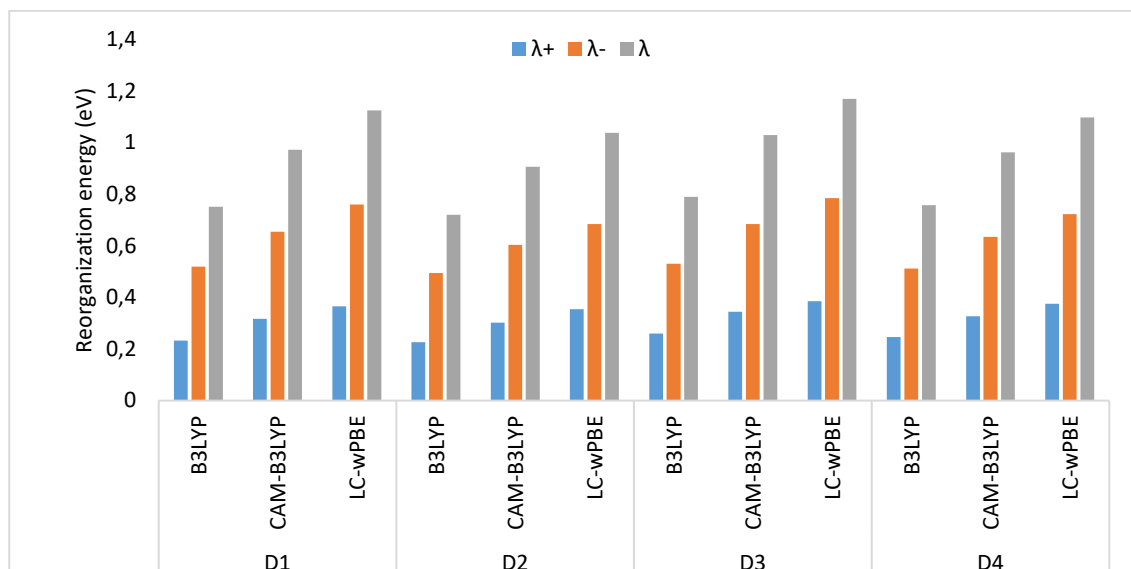
Fig. 5. The calculated reorganization energies (λ^+, λ^-, and λ) for studied dyes with different functionals.

3.4 Absorption spectra

In Table 3, we have presented the values of the calculated absorption maxima of the studied compounds and the experimental value of the dye D1, to find the most suitable method which gives a good description of the optical properties of the studied molecules and which can be employed to predict the characteristics of other materials. For this, we used different functionals that are B3LYP, CAM-B3LYP, LC-wPBE and BHandHLYP.

The density functionals BHandHLYP and CAM-B3LYP are quasi-similar for D1 with a margin of about 14 nm comparing with the experimental value, while the absorption wavelengths of LC-ωPBE and B3LYP (405.17 and 593.96 nm) are significantly lower and higher, respectively, than the experimental value. The reason for this difference should be the result of the difference in the electron density approximation methods of different density functionals. To evaluate the overall performance of the studied functionals,

we refer to the mean absolute error (MAE) calculated for the three main absorption bands in UV-Vis for D1. It is calculated as follows [34]:

$$MAE = \frac{1}{n}\sum_{i=1}^{n}\left|\lambda_i^{calc.} - \lambda_i^{expt.}\right|, n = 3$$

The MAEs of the DFT functionals are given in Table 3.

From Table 3, we note that the highest MAE value is that of the B3LYP functional (MAE = 75 nm), which indicates low precision for this hybrid functional in the prediction of optical properties. On the other hand, MAEs of long-range corrected DFT functional (LC), (CAM-B3LYP and LC-wPBE) suggest the latter as suitable models in the prediction of optical properties of organic dyes, the good performance of this type of functional is due to the presence of the terms of separation of scope and corrections of dispersion [34]. The results of Table 2 then show that the effect of functional change depends on the percentages of HF exchange and correlation.

On the other hand, as shown in fig.6, in terms of absorption peak wavelength, the calculation result of B3LYP has the strongest maximum absorption compared with the experimental value, and the absorption peak intensity tends to be overestimated for all studied dyes. For this reason, we can note that the TD-B3LYP model produces the least accurate results in the table, indicationg B3LYP hybrid functional as

unable to produce spectral band positions with sufficient accuracy. This may be attributed to the excessive energy stabilization due to delocalization error of this functional when the chemical system has fractional electron numbers in the frontier orbitals. However, the density functional results of CAM-B3LYP and BHandHLYP are compared Similar (< 7 nm) for all studied dyes. We also noted that the density functional results of B3LYP have a significant red shift comparing with other XC functionals, while the LC-ωPBE density functional results have a blue shift.

Previously, it has been demonstrated that the BHandHLYP hybrid functional reproduces maximum absorption of D1 molecule very well. At the same time, in our calculations, the long-range-corrected density functional, CAM-B3LYP, estimates the maximum absorption of D1 as well as the BHandHLYP functional. As a result, we can conclude that these two funcationals have the best slope performance of maximum absorption and are in good agreement with the experimental values.

We can also note that the optical parameters are affected by the nature of the π-spacer of the studied dyes. It can be observed that D3 is characterized by the highest absorption maximum (λ_{max}) involving a high light harvesting capability. This can be explained by the strong conjugation between the withdrawing group and the thiazole unit.

Table 3. The maximum absorption wavelengths (λ_{max}/nm), oscillator strengths (f), light harvesting efficiency (LHE) and the mean absolute error, of studied dyes, computed in THF using BHandHLYP, B3LYP, CAM-B3LYP and LC-wPBE functionals at TD-functional/6-31+G(d) level.

| Dyes	Functionals	f	λ_{max}			MAE	LHE
			λ_1	λ_2	λ_3		
D1	BHandHLYP	1.305	456.26	325.31	297.96	22	0.950
	B3LYP	0.894	593.96	392.37	363.21	75	0.872
	CAM-B3LYP	1.308	457.47	457.47	307.94	30	0.951
	LC-wPBE	1.402	405.17	291.79	281.23	49	0.960
	Expt*		443	382	301		
D2	BHandHLYP	1.240	428.26				0.942
	B3LYP	0.747	554.93				0.821
	CAM-B3LYP	1.230	432.89				0.941
	LC-wPBE	1.265	396.74				0.946
D3	BHandHLYP	1.150	487.33				0.929
	B3LYP	0.718	659.35				0.808
	CAM-B3LYP	1.162	482.43				0.931
	LC-wPBE	1.318	411.03				0.952
D4	BHandHLYP	1.107	446.32				0.922
	B3LYP	0.615	612.44				0.757
	CAM-B3LYP	1.114	445.62				0.923
	LC-wPBE	1.232	392.73				0.941
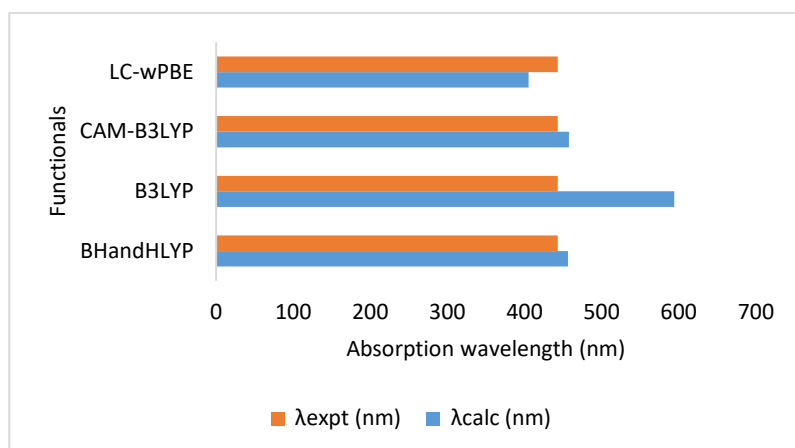
Fig. 6 The correlation plot of the calculated vs experimental absorption wavelength for the dye D1 with different functional.

In this context, it may be noted that the molecular structure that exhibits a conjugation between a heterocycle based on sulfur and oxygen atoms and the donor-acceptor system, improves the conjugation of organic sensitizers and stabilize them.

The comparison of these different optical properties shows that by simple structural modification of dyes otherwise part of the D-π-A push-pull structure, it is possible to improve the conversion efficiencies of dye-sensitized solar cells.

4. Conclusions

This study, we evaluated four functional, which are B3LYP, CAM-B3LYP, LC-wPBE and BHandHLYP in the calculation of structural, optoelectronic and charge transfer properties of organic dyes. Calculations are performed using Density Functional Theory (DFT) and Time Dependent Density Functional Theory (TD-DFT).

By referring to an experimental study already carried out on the energy gap of one of the studied molecules, the calculations revealed that the hybrid functional B3LYP is the most suitable for predicting the geometric and electronic properties of the organic studied dyes.

On the other hand, we have shown that the BHandHLYP functional with a percentage of 50% HatreeFock exchange gave good results for the optical properties in good agreement with the experimental data. In addition, the corrected long-range functionals were also successful in predicting the optical properties in particular the CAM-B3LYP functional.

In conclusion, it seems obvious that the choice of the adequate functional is important for the determination of sensitizers' properties. In this context, our results show that the level of theory we have chosen allows us to find the experimental data. The computational methodology can therefore be used to predict the optoelectronic properties of other organic compounds and to design future materials to be applied in DSSCs.

Supporting Information

Cartesian coordinates.

Acknowledgments

Author Contributions

ML did most of the practical work as part of a PhD thesis supervised by HT and prepared the manuscript. HT designed and coordinated the study, participated in article preparation, corrected the manuscript and edited the final version and submitted it for publication. SE contributed to data analysis. FL and SMB participated in study designed, helped to improve the manuscript and critically revised the manuscript. All authors read and approved the final manuscript.

References and Notes

[1] Tai, C. K.; Hsieh, C. A.; Hsiao, K. L.; Wang, B. C.; Wei Y. *Organic Electronics* **2015**, *16*, 54. **[Crossref]**

[2] El Assyry, A.; Lamsayah, M.; Warad, I.; Touzani, R.; Bentiss, F.; Zarrouk, A. *Heliyon* **2020**, *6*, 3620. **[Crossref]**

[3] Üngördü, A. *Chem. Phys. Lett.* **2019**, *733*, 136696. **[Crossref]**

[4] Tiwari, A.; Kumar, B.; Srivastava, A. K. *Mater. Today: Proc.* **2020**, *29*, 772. **[Crossref]**

[5] Surukonti, N.; Kotamarthi, B. *Comput. Theor. Chem.* **2018**, *1138*, 48. **[Crossref]**

[6] Zaier, R.; Hajaji, S.; Kozaki, M.; Ayachi, S. *Opt. Mater.* **2019**, *91*, 108. **[Crossref]**

[7] Amkassou, A.; Zgou, H. *Mater. Today: Proc.* **2019**, *13*, 569. **[Crossref]**

[8] Erdogdu, Y.; Baskose, U. C.; Saglam, S.; Erdogdu, M.; Ogutcu, H.; Özçelik, S. *J. Mol. Struct.* **2020**, *1221*, 128873. **[Crossref]**

[9] Ocakoglu, K.; Sogut, S.; Sarica, H.; Guloglu, P.; Erten-Ela, S. *Synth. Met.* **2013**, *174*, 24. **[Crossref]**

[10] Qin, C.; Clark, A. E. *Chem. Phys. Lett.* **2007**, *438*, 26. **[Crossref]**

[11] Tai, C. K.; Chen, Y. J.; Chang, H. W.; Yeh, P. L.; Wang, B. C. *Comput. Theor. Chem.* **2011**, *971*, 42. **[Crossref]**

[12] Jones, R. O. *Rev. Mod. Phys.* **2015**, *87*, 897. **[Crossref]**

[13] Baseden, K.A.; Tye, J. W. *J. Chem. Educ.* **2014**, *91*, 2116. **[Crossref]**

[14] Hohenberg, P. C.; Kohn, W.; Sham, L. J. *Adv. Quantum Chem.* **1990**, *21*, 7. **[Crossref]**

[15] Kohn W.; et Sham, L. J. *Phys. Rev.* **1965**, *140*, A1133. **[Crossref]**

[16] Langreth, D. C.; Mehl, M. J. *Phys. Rev. B* **1983**, *28*, 1809. **[Crossref]**

[17] Becke, A. D. *Phys. Rev. A.* **1988**, *38*, 3098. **[Crossref]**

[18] Perdew, J. P. *et al. Phys. Rev. B.* **1992**, *46*, 6671. **[Crossref]**

[19] Miroshkina, O. N. *et al. J. Appl. Phys.* **2020**, *127*, 175108. **[Crossref]**

[20] Ernzerhof, M.; Scuseria, G. E. *J. Chem. Phys.* **1999**, *110*, 5029. **[Crossref]**

[21] Tsuneda, T.; Hirao, K. *Wiley Interdiscip. Rev.: Comput. Mol. Sci.* **2014**, *4*, 375. **[Crossref]**

[22] Fritsch, D.; Morgan, B. J.; Walsh, A. *Nanoscale Res. Lett*. **2017**, *12*, 19. **[Crossref]**

[23] Lazrak, M.; Toufik, H.; Bouzzine, S. M.; Lamchouri, F. *Res. Chem. Intermed.* **2020**, *46*, 3961. **[Crossref]**

[24] Fahim, Z. M. E.; Bouzzine, S. M.; Youssef, A. A.; Bouachrine, M.; Hamidi, M. *Comput. Theor. Chem.* **2018**, *1125*, 39. **[Crossref]**

[25] Fehér, P. P.; Purgel, M.; Joó, F. *Comput. Theor. Chem.* **2014**, *1045*, 122. **[Crossref]**

[26] Available from: **https://gaussian.com/g09citation/.** Access October 2019.

[27] Corà *, F. *Mol. Phys.* **2005**, *103*, 2483. **[Crossref]**

[28] Yanai, T.; Tew, D. P.; Handy, N. C. *Chem. Phys. Lett.* **2004**, *393*, 51. **[Crossref]**

[29] Vydrov, O. A.; Scuseria, G. E. *J. Chem. Phys.* **2006**, *125*, 234109. **[Crossref]**

[30] Wang, C. W.; Hui, K.; Chai, J. D. *J. Chem. Phys.* **2016**, *145*, 204101. **[Crossref]**

[31]   Sharma, D.; Paterson, M. J. *Photochem. Photobiol. Sci.* **2014**, *13,* 1549. **[Crossref]**

[32]   Stephens, P. J.; Devlin, F. J.; Chabalowski, C. F.; Frisch, M. J. *J. Phys. Chem.* **1994**, *98*, 11623. **[Crossref]**

[33]   Balanay, M. P.; Kim, D. H. *J. Mol. Struct.: THEOCHEM* **2009**, *910*, 20. **[Crossref]**

[34]   Mohammadi, N.; Wang, F. *J. Mol. Model.* **2014**, *20*, 2177. **[Crossref]**

How to cite this article